Механика материалов: прочность, ресурс, безопасность

Materials mechanics: strength, durability, safety

DOI: https://doi.org/10.26896/1028-6861-2020-86-5-43-51

REGULARITIES AND PROPERTIES OF INSTRUMENTED INDENTATION DIAGRAMS OBTAINED BY BALL-SHAPED INDENTER

- © Vyacheslav M. Matyunin^{1*}, Artem Yu. Marchenkov¹, Nuha Abusaif², Pavel V. Volkov¹, Daria A. Zhgut¹
- National research university "Moscow Power Engineering Institute", 14, Krasnokazarmennaya ul., 111250, Moscow, Russia, *e-mail: MatiuninVM@mpei.ru
- ² Tishreen University, POB 1385, Lattakia, Syria.

Received December 20, 2019. Revised January 17, 2020. Accepted February 20, 2020.

The history of appearance and the current state of instrumented indentation are briefly described. It is noted that the materials instrumented indentation methods using a pyramid and ball indenters are actively developing and are currently regulated by several Russian and international standards. These standards provide formulas for calculating the Young's modulus and hardness at maximum indentation load. Instrumented indentation diagrams "load F – displacement α " of a ball indenter for metallic materials were investigated. The special points on the instrumented indentation diagrams " $F - \alpha$ " loading curves in the area of elastic into elastoplastic deformation transition, and in the area of stable elastoplastic deformation are revealed. A loading curve area with the load above which the $dF/d\alpha$ begins to decrease is analyzed. A technique is proposed for converting " $F - \alpha$ " diagrams to "unrestored Brinell hardness HB_t - relative unrestored indent depth t/R" diagrams. The elastic and elastoplastic areas of " $HB_t - t/R$ " diagrams are described by equations obtained analytically and experimentally. The materials strain hardening parameters during ball indentation in the area of elastoplastic and plastic deformation are proposed. The similarity of " $HB_t - t/R$ " indentation diagram with the "stress σ – strain δ " tensile diagrams containing common zones and points is shown. Methods have been developed for determining hardness at the elastic limit, hardness at the yield strength, and hardness at the ultimate strength by instrumented indentation with the equations for their calculation. Experiments on structural materials with different mechanical properties were carried out by instrumented indentation. The values of hardness at the elastic limit, hardness at the yield strength and hardness at the ultimate strength are determined. It is concluded that the correlations between the elastic limit and hardness at the elastic limit, yield strength and hardness at the yield strength, ultimate tensile strength and hardness at the ultimate strength is more justified, since the listed mechanical characteristics are determined by the common special points of indentation diagrams and tensile tests diagrams.

Keywords: instrumented indentation; ball indenter; hardness; mechanical characteristics; indentation diagrams; strain hardening.

Introduction

A new stage in the indentation hardness test began with the appearance of the devices and methods, which allow obtaining the "load - displacement" diagrams. This type of indentation test was known as "instrumented indentation." Earlier in Russia, another expression was proposed — "kinetic indentation." This term is substantiated by the fact that during such type of indentation it is possible to obtain information about the kinetics processes of material deformation under loading and unloading processes. When an indenter is loaded, the material experiences elastic and elastoplastic deformation. For low plasticity materials, the elastoplastic deformation stage can transform into the fracture stage and cracks around the indent will be formed. All elastic, elastoplastic deformation, relaxation and fracture processes are shown on the instrumented indentation diagram in

the form of separate sections, inflection points or fractures.

Based on the literature analysis it can be noted that the information about instrumented indentation diagrams and first devices was first introduced in 1952-1953 by P. Grodzinski [1, 2], 1967-1968 by G. N. Kaley [3, 4], 1970-1972 by M. P. Markovets and his colleagues [5-7], 1971-1975 by V. P. Alekhin, S. I. Bulychev, et al. [8-10].

In these publications were demonstrated instrumented indentation diagrams, which were obtained by using various shapes of the indenter (ball, pyramid, and cone) in macro- and micro indentation scale. In subsequent years, the instrumented indentation test was developed based on more advanced means of information measuring and computer technology. It became possible to obtain an indentation diagram in the nano scale, which is necessary for measuring the mechanical

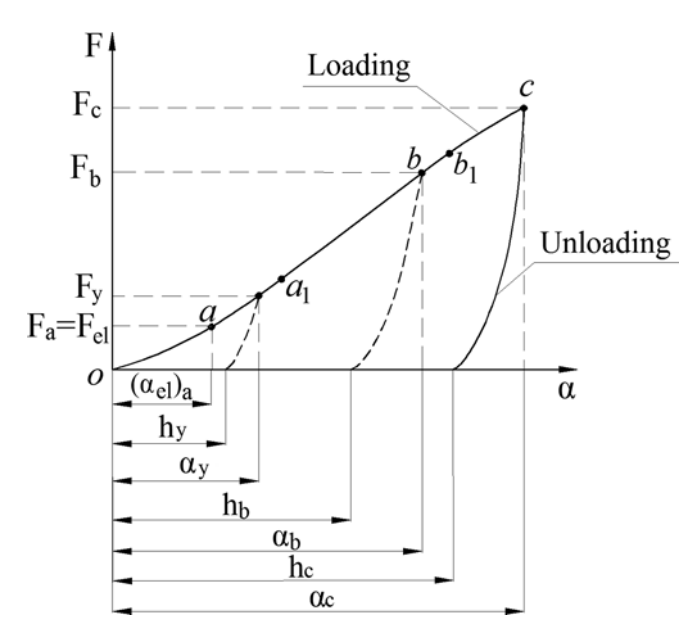


Fig. 1. Ball indentation diagram " $F - \alpha$ " with loading and unloading curves

properties of materials surface layers, coatings, and thin membranes. These achievements are described in a lot of scientific articles and monographs, for example, in [11-19].

Nowadays the instrumented indentation methods by using a pyramid and ball indenters are regulated by several standards [20 - 24]. These standards present methods for determining the hardness and elastic modulus using the instrumented indentation diagram, but in the Russian standard [21] additionally are provided recommendations for converting the ball instrumented indentation diagram in the coordinates "load - displacement indenter" to a tensile diagram in the coordinates "stress - strain." However, in the practical use of existing standards, difficulties may occur during instrumented indentation diagrams analysis and determination of the hardness and elastic modulus for materials with an unknown level of physical and mechanical properties. In addition, the determination results of these mechanical characteristics, especially the elastic modulus, strongly depend on the device elastic compliance. Therefore, many methods have been proposed to evaluate the device elastic compliance, each of these methods has its advantages and disadvantages [22, 25].

The primary instrumented indentation diagram with ball indenter in the coordinates "load F – indenter displacement α " can be converted to a diagram in the coordinates "contact stress — contact strain" [19]. This diagram allows developing a more reasonable method for converting it into a tensile diagram in the "stress – strain" coordinates. However, in this case, it is necessary to have a reasonable relationship between the indentation

strains and the tensile strains by taking into account the physical, mechanical and geometric similarity conditions. At the same time, it is important to study the indentation size effect which impacts on the mechanical characteristics of materials. Such characteristics can be evaluated by tensile and indentation methods [19].

It should be noted that the undiscovered possibilities of ball-instrumented indentation can expand the range of mechanical characteristics, which can be determined by indentation diagrams.

Based on this, the paper presents the research results of regularities and characteristics of ball instrumented indentation diagram for structural materials with different mechanical properties and proposes new methods to convert these diagrams and use them to determine the elastic modulus, strain hardening parameters and hardness characteristics at different stages of elastoplastic deformation.

Figure 1 shows a ball indentation diagram "F – α " with loading and unloading curves. Authors consider that complete indentation diagrams include elastic and elastoplastic deformation areas with an excess of the indentation load at which an inflection occurs in point b_1 , and then a decrease in the dF/d α also occurs.

This diagram represents an instrumented indentation diagram for metal with medium hardness and plasticity. The initial part of the diagram oa corresponds to the elastic deformation area of the tested material, the indenter and other loaded parts of the device. The elastic area ends in point a, with a load $F_a = F_{el}$ and a total elastic displacement is $(\alpha_{el})_a$.

After a complete unloading, the unloading curve of the indentation diagram coincides with the loading curve and returns to zero. However, if the indentation diagram " $F - \alpha$ " is registered with ball diameter D = 1 - 10 mm, the elastic area is difficult to identify because of its small extent. For this, larger diameters of indenters are required D if the typical medium hardness materials are used. Figure 2 shows the elastic region of the ball instrumented indentation diagram (D = 15 mm)" $F - \alpha$ " for 35KhVFYuA steel. This diagram was recorded by an Instron 5982 machine. The loading and unloading curves of this diagram coincide (shown by arrows), which confirms the presence of only elastic deformation. In Fig. 2 by a dashed line, another indentation diagram is also shown in coordinates "load F – elastic displacement α_0 ." The elastic displacement α₀ consists of the elastic deformation of both the tested material and the ball.

This diagram " $F - \alpha_0$ " reproduces the theoretical dependence of H. Hertz [24]:

$$F = \frac{4R^{0.5}}{3\left(\frac{1-v_m^2}{E_m} + \frac{1-v_i^2}{E_i}\right)}\alpha_0^{1.5} = \alpha_0\alpha_0^{1.5}, \tag{1}$$

where

$$a_0 = \frac{4R^{0.5}}{3\left(\frac{1 - v_m^2}{E_m} + \frac{1 - v_i^2}{E_i}\right)},$$
 (2)

R — the indenter radius, v_m and v_i are the Poisson ratios, E_m and E_i are elastic modulus of the tested material and the indenter.

The large difference in the arrangement of curves 1 and 2 in Fig. 2 is caused by the strong influence of the device elastic compliance. If curve 1 includes the elastic deformation of the ball and the tested material, then curve 2 add elastic deformations information of the device component.

Therefore, for accurate determination of the tested material elastic deformation, it is necessary to take into account the device elastic compliance. The authors of this paper used various existing methods for evaluating the device elastic compliance. Based on the obtained experience, a new method was proposed [25], which is based on H. Hertz equation (1), the meaning of which is illustrated in Fig. 2. While the load F increases, $\Delta \alpha = \alpha_{el} - \alpha_0$ rises too. Between $\Delta \alpha$ and F there is a clear dependence, which is special for each device. Therefore, knowing this dependence at any given load F, $\Delta \alpha$ can be determined.

It should be noted that the elastic modulus, which is determined by the diagram " $F-\alpha$," is considered to be a criterion for the accurate evaluation of the device elastic compliance. If the elastic modulus values, which are determined by indentation and tensile methods are the same or close enough, so this confirms about the correctness of the selected method for estimation the devise elastic compliance.

With a small excess of the load F_a (Fig. 1), a smooth bending of the loading curve occurs in the transition zone $a-a_1$ from elastic deformation into elastic-plastic, and after completely unloading, the unloading curve will not return to the zero due to the small plastic deformation. In the transition deformation zone on the loading curve, there is a point at which the load F_y corresponds to the yield strength with a given limit for residual deformation (see Fig. 1).

With an increase of the indentation load to F_b , the intensive hardening of the tested material occurs, which is confirmed by an $dF/d\alpha$ increasing.

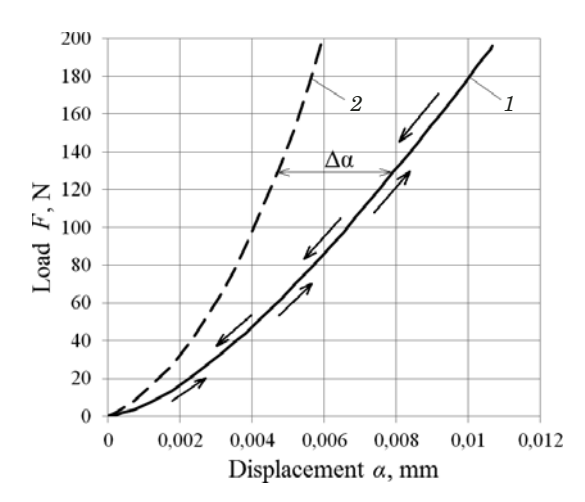


Fig. 2. Indentation diagrams " $F-\alpha_{el}$ " (1) and " $F-\alpha_0$ " (2) in the elastic region of ball indentation ($D=15~\rm mm$) for $35\rm KhVFYuA$ steel

However, in region $b-b_1$, the loading curve becomes almost straight, and the $\mathrm{d}F/\mathrm{d}\alpha$ remains constant. The extent of the region $b-b_1$ can vary greatly for different materials. It was found that with growing the ultimate uniform deformation of the tested material, this section also increases. For materials with a small ultimate uniform deformation (less than 3%), the length of section $b-b_1$ becomes insignificant, and the points b and b_1 are almost coincide.

As the indentation load rises to F_{b1} , another smooth bend of the loading curve occurs, and the d $F/d\alpha$ begins to gradually decrease. At the end of the diagram " $F-\alpha$ " when $F=F_c$, the total elastoplastic indenter displacement α_c is:

$$\alpha_c = h_c + (\alpha_{el})_c + (\Delta \alpha_{el})_c, \tag{3}$$

where h_c — residual indent depth, which is independent of the device elastic compliance; $(\alpha_{el})_c = \alpha_c - h_c$ — elastic component of the general elastoplastic indenter displacement; $(\Delta\alpha_{el})_c$ — additional elastic deformation of the device at load F_c .

A similar separation of the general indenter displacement can be performed for points b and b_1 by complete unloading. Figure 3 shows the diagrams " $F-\alpha$ " for several different structural materials.

These diagrams were obtained by ball instrumented indentation with a diameter D=1 mm, because of this the elastic regions are very small and impossible to distinguish and the inflection of the loading curve in point a is also very difficult to identify. At the same time, if the presence of inflection in point a can be explained by the transition of elastic deformation into elastoplastic, then the inflection in point b requires a separate explanation and experimental basis. It can be assumed that as the load increases to F_b , more significant elastic

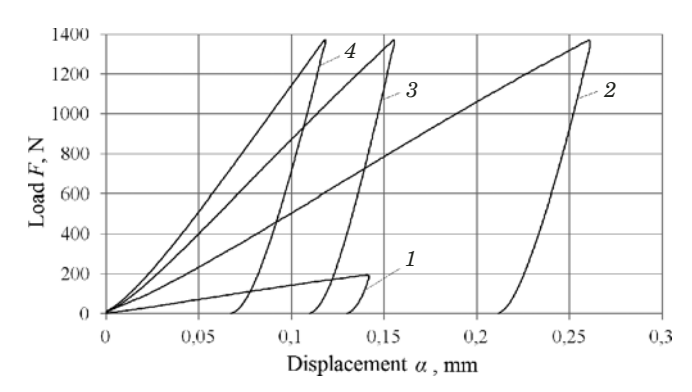


Fig. 3. Indentation diagrams " $F - \alpha$ " for several materials: I - AMTs; 2 - EP17; 3 - 35HVFYuA; 4 - EI474

pressure of the ball occurs, which changes ball geometry and radius in the contact area. However, experiments show that the load values F_b can vary greatly for different materials at the same R. For example, when ball instrumented indentation with R = 0.5 mm was carried out on an AMTs magnesium alloy with a hardness 35.5HB, the load F_b was 49 N (5 kgf) and for 35HVFYuA steel with a hardness 325HB, the load F_b reached 1177 N (120 kgf). When a load is 49 N (5 kgf), the elastic pressure of the steel hardened ball is negligible and it cannot affect its geometry. The presented data indicate that the geometrical factor, as the cause of inflection in the point bl in the diagram " $F - \alpha$ " is excluded. Consequently, when point b_1 is reached, the elastoplastic deformation stability is violated and then a decrease in the material hardenability is occurred, which leads to a decrease in the $dF/d\alpha$. Furthermore, as will be shown below, at a load F > $> F_b$, the Brinell hardness values begin to decrease.

Convert of diagrams " $F - \alpha$ " to diagrams " $HB_t - t/R$ "

Indentation diagrams "unrestored Brinell hardness HB – relative unrestored indent depth t/R" allow more reasonably to establish their relationship with tensile diagrams "conditional stress σ — conditional relative elongation δ " [19]. Considering that, the ratio t/R characterizes the average contact deformation and HB_t is the average contact pressure when the ball is pressed in, then the analogy between the diagrams " $HB_t - t/R$ " and " $\sigma - \delta$ " is clear. The main goal in converting the " $F - \alpha$ " diagram to the " $HB_t - t/R$ " diagram is to determine the unrestored indent depth in the elastic and elastoplastic indentation areas.

In the elastic indentation area on the part oa, the elastic indent depth t_{el} is:

$$t_{el} = \gamma(\alpha_0), \tag{4}$$

where $\gamma = E_i/(E_i + E_m)$.

When $E_i = E_m$ so $\gamma = 0.5$, and t_{el} will be equal to:

$$t_{el} = \alpha_0/2. \tag{5}$$

In the elastoplastic indentation area t is:

$$t = h + \gamma(\alpha - h), \tag{6}$$

where $\gamma(\alpha - h)$ — the elastic component t, h — the residual indentation depth.

When $E_i = E_m$, equation (6) takes the form:

$$t = (\alpha + h)/2. \tag{7}$$

Thus, to determine t at a given load F, it is necessary to know E_i , E_m , α , and h. Having the elastic part of the diagram " $F-\alpha$," E_m can be calculated, based on equation (1). For this, it is additionally needed to know v_i and v_m . If E_m is unknown, the elastic area of the diagram " $F-\alpha$ " cannot be clearly identified, so to determine the E_m , the elastoplastic area of the diagram " $F-\alpha$ " can be used with the determination of the elastic component α_{el} at a final load F. Before it, a complete unloading must be performed to determine h. However, in this case, α_{el} will be different from α_0 , which is calculated by equation (1) due to the influence of plastic deformation. This influence can be taken into account by the correction λ [26]:

$$\lambda = \left(1 + \frac{2h}{\alpha_{el}}\right)^{1/3}.$$
 (8)

Then

$$\alpha_0 = \Delta \alpha_{el}. \tag{9}$$

From (1), with considering (8) and (9), it is possible to obtain [27]:

$$E_{m} = \frac{1 - v_{m}^{2}}{\frac{4(\alpha - h)\sqrt{R(\alpha + h)}}{3F} - \frac{1 - v_{i}^{2}}{E_{i}}}.$$
 (10)

Experiments, which were performed on steels, aluminum, magnesium, and titanium alloys showed that the relative digression of the E_m values, which were determined by the indentation method by equation (10) and tensile method on the same sample does not exceed 10% [25].

For determining the h values at each point of the elastoplastic part of the diagram " $F-\alpha$," two methods can be used. The first method consists of repeatedly loading the indenter to different loads and then unloading it. Figure 4 shows a step diagram of ball indentation for steel 45 with repeated loading and complete unloading. The more loading

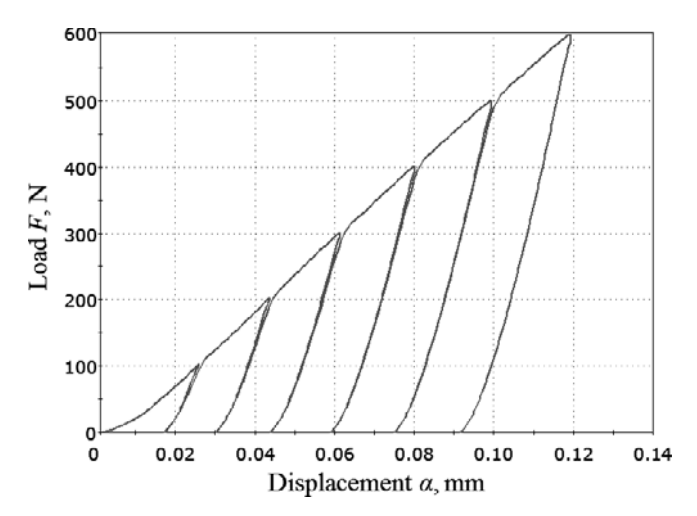


Fig. 4. Step diagram of ball indentation for steel 45 with loading and unloading curves (D = 1 mm)

and unloading stages are obtained, the greater the number of h values will be determined.

There is also another method for determining h. It is known that at a certain initial part of the indentation plastic region when a ball is used, a linear dependence between F and h is observed, which was first established by A. Martens. According to this, by extrapolating the dependence to small loads and indent depths, it passes through the origin. However, according to [26], for some materials with such extrapolation, the straight line may not pass through the origin, cutting off a very small section along the F axis. At the same time, based on research results, which were performed earlier by the authors of this article [28] and in the present work for metallic materials with various mechanical properties and microstructure, the extrapolated straight line passed clearly through the origin, which allows it to be described by A. Martens equation:

$$F = kh, \tag{11}$$

where k — constant-coefficient for the tested material, which characterizes its hardenability in the indentation plastic area.

Figure 5 shows diagrams "F - h," which were obtained by the step diagrams " $F - \alpha$ " for three different samples from steel using an Instron 5982 machine. The dashed lines indicate the extrapolated linear sections in the lower part of the diagrams, which pass through the origin, as well as in the upper part of the diagrams.

At the same time, as the indentation load increases in the area of development plastic deformations, the curvature of straight lines occurs, which is accompanied by a decrease in the coefficient k. Our experiments showed that the relative residual indent depth h/R, at which the straightness of the

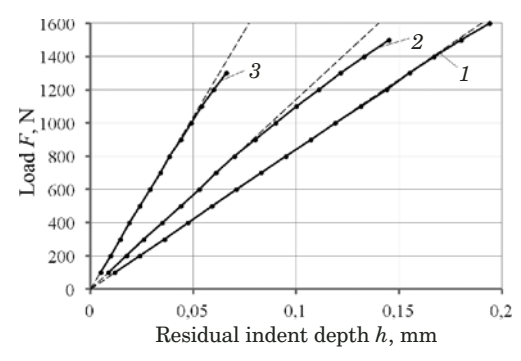


Fig. 5. Indentation diagrams "F - h" in the plastic region for materials: I - 10Kh18N10T; 2 - 25Kh2MFA; 3 - 25Kh2MF

diagram "F-h" is violated, the greater is, the higher the ultimate uniform deformation when the sample is broken. For steel 10Kh18N10T with high uniform deformation, the straightness of the diagram is maintained up to $h/R \approx 0.35$. In addition, it was found that for the tested materials, the maximum load to which the straightness of the diagram "F-h" is saved is close to the load, which corresponds to point b in the " $F-\alpha$ " diagram (Fig. 1). Therefore, by determining h at the load $F_{a1} \leq F \leq F_b$, the coefficient k for the tested material can be found and then use to determine h for any given load in the interval $F_{a1}-F_b$.

It should be noted that the coefficient k depends on the indenter radius; when the same material is tested if the R decreases, the k will decrease too. However, if k is expressed from equation (11) and then is divided by R, then the hardening parameter q will be obtained, which remains constant at macro indentation levels with different R:

$$q = \frac{F}{hR}. (12)$$

If q is divided by the elastic moduli of the tested material E_m , the dimensionless strain hardening coefficient q' will be obtained in the plastic deformation area:

$$q' = \frac{F}{hRE_m}. (13)$$

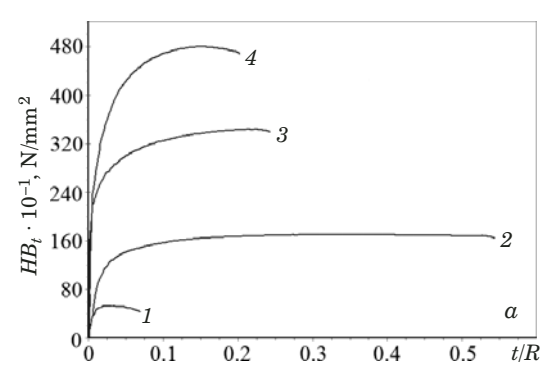
Thus, the residual indentation depths at given loads F in the interval $F_{a1} - F_b$ can be calculated from q or q':

$$h = \frac{F}{qR} = \frac{F}{q' E_m R}.$$
 (14)

In the elastic indentation area oa, the load dependence F on elastic indentation depth from (1) and (4) is given by:

$$F = c_1 t_{\rho l}^{1.5}, \tag{15}$$

where $c_1 = \alpha_0/\gamma$.



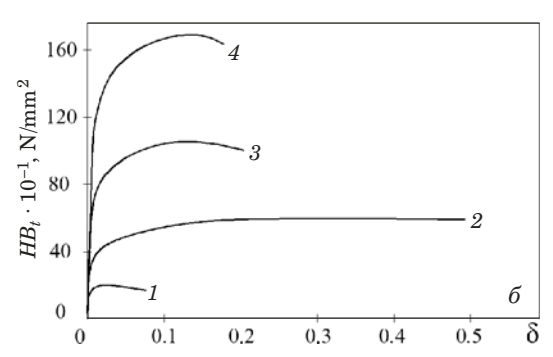


Fig. 6. Indentation diagrams " $HB_t - t/R$ " (a) and tension diagrams " $\sigma - \delta$ " (b) for different materials: 1 - AMTs; 2 - EP17; 3 - 35KhVFYuA; 4 - EI474

In the elastoplastic indentation area a_1b , the load dependence F on t can be approximated by the power equation [19]:

$$F = at^n, (16)$$

where a and n are coefficients for the tested material.

The coefficient n is a parameter of strain hardening in the elastoplastic deformation area. Its value can be determined by regression analysis of the "F-t" array in the area of a_1-b on the loading curve. Table 1 shows the values of strain hardening parameters q, q', n, as well as the elastic modulus E_m and the coefficients a_0 , a, and γ for several structural materials.

Having the F and t values, the unrestored Brinell hardness values HB_t can be calculated as:

$$HB_t = \frac{F}{2\pi Rt}. (17)$$

In the elastic indentation area oa, the HB_t dependence on t/R from (6) and (17) is given by:

$$HB_t = b(t/R)_{el}^{0.5},$$
 (18)

where $b = a_0/(2\pi R^{0.5} \gamma^{1.5})$.

In the elastoplastic indentation area a_1b , the HB_t dependence on t/R follows from (16) and (17):

$$HB_t = c(t/R)^{n-1}, \tag{19}$$

where $c = aR^{n-2}/(2\pi)$.

Thus, equations (18) and (19) describe the indentation diagram " $HB_t - t/R$ " in the elastic (oa) and elastoplastic deformation (a_1b) areas.

Figure 6*a* shows indentation diagrams " $HB_t - t/R$ " for different materials, which were obtained on a device MEI-TA using a ball with a diameter D = 1 mm.

In these diagrams, the peak is clearly visible, where the hardness HB_t reaches its maximum value (HB_t) u, after which it decreases. At the area of high point (see $b - b_1$ area in Fig. 1), the HB_t values change insignificantly, as a result, a horizontal line is formed, the length of which is the greater, the higher the ultimate uniform deformation. Therefore, for example, for EP17 steel with a high ultimate uniform deformation, this line is the longest in comparison with other materials. It should be noted that a similar prolonged maximum in the form of a horizontal line is also observed in the " $\sigma - \delta$ " diagram of this material (Fig. 6b). Therefore, to determine the coordinates of the point where the highest HB_t value will actually be, highprecision loads and displacements measurements are required for both types of deformation, which were obtained by indentation and tensile methods.

Thus, the " $HB_t - t/R$ " indentation diagrams and the " $\sigma - \delta$ " tension diagrams have similarities and common characteristic zones and points in different elastic and elastoplastic deformation stages. By virtue of analogy with tension diagrams, indentation diagrams can be used to find points corresponding to hardness at the elastic limit, hardness

Table 1. Elastic modulus and instrumented indentation parameters, which were determined in the elastic and elastoplastic deformation areas for structural materials ($R=0.5~\mathrm{mm}$, $E_i=211,000~\mathrm{N/mm^2}$, $v_m=v_i=0.3$)

Material	$\begin{array}{c} E_m, \mathrm{N/mm^2,} \\ \mathrm{Eq.} \ (10) \end{array}$	a_0 , N/mm ^{3/2} , Eq. (2)	γ, Eq. (4)	n	a , N/mm n	q, N/mm², Eq. (12)	q', Eq. (13)
AMTs	75,046	57,389	0.738	1.070	1766	3396	0.0453
15Kh1M1F	211,403	109,554	0.499	1.095	6566	10,703	0.0506
Steel 50	204,097	107,627	0.508	1.068	8633	16,107	0.0789
35KhVFYuA	205,688	108,052	0.506	1.130	14,597	21,420	0.1041

at the yield strength and hardness at the ultimate strength, which will be described below.

Hardness determination at the elastic limit, at the yield strength, and at the ultimate strength

The idea of hardness determination at the elastic limit during ball indentation belongs to H. Hertz [29], who proposed to call it "absolute hardness." H. Hertz take into consideration that absolute hardness has a special physical meaning and it characterizes the material resistance to the ball elastic indentation. After the indentation load is completely removed, the elastically deformed material returns to its initial state, and reversible plastic deformation and the strain hardening do not affect the hardness-determined value.

However, the evaluation of absolute hardness or hardness at the elastic limit by measuring the elastic indent dimensions is rather difficult.

A simpler method was proposed by G. P. Zaitsev [30]. This method based on the H. Hertz equation, which establishes the relation between the indentation load and the elastic indentation diameter, and on the E. Meyer equation, which establishes the relation between the indentation load and the residual indentation diameter. In the joint solution of these two equations, the equation for evaluation of the indent diameter at the elastic limit can be obtained and then used to evaluate the hardness at the elastic limit. At the same time, in this method, there is a controversial assumption, which considers that the elastic and residual indent diameters are equal at one indentation load in the area of elastic into elastoplastic deformation transition.

Methods for determining hardness at the elastic limit were analyzed in [31] and a proposal was made to use ball instrumented indentation for this purpose. To do this, H. Hertz's equation (1) was also applied, which establishes the relation between the indentation load and the elastic displacement α_0 and the power dependence (16) of the indentation load on the elastoplastic displacement α_0 . As a result, an equation for evaluating the hardness at the elastic limit by the elastic displacement and independence on the elastic indentation depth was obtained. In the joint solution of equations (18) and (19) a more reasonable equation for evaluation the hardness at the elastic limit $(HB_t)_{el}^*$ can be achieved:

$$(HB_t)_{el}^* = \frac{a_0^{\frac{n-1}{n-1.5}}}{2\pi Ra^{\frac{0.5}{n-1.5}}\gamma^{\frac{0.5(n-1)}{n-1.5}}}.$$
 (20)

Another approach to evaluating hardness at the elastic limit $(HB_t)_{el}^*$ by instrumented indentation method is to study a small plastic deformation, for example, equal to 0.0005 = 0.05%, by analogy with the method for evaluating the elastic limit $\sigma_{0.05}$ from the tension diagram of the tested material. In this regard, important studies were carried out in [32] using the M. P. Markovets equation [11] for evaluating the average contact deformation $\psi^{\rm in}$ when the ball is pressed:

$$\psi^{in} = \frac{1}{2} \left[1 - \sqrt{1 - \left(\frac{d}{D}\right)^2} \right].$$
(21)

Moreover, in this case, it was assumed that the residual indent depth $h_{0.05}=0.0005D$. However, when $\psi^{\rm in}=0.0005$ is substituted in the equation (21), the indent diameter $d_{0.05}=0.0447D$ can be determined. If this diameter is evaluated, then $t_{0.05}=0.0005D$ will be obtained. However, this will be the unrestored indent depth $t_{0.05}$, which is always greater than the residual indent depth $h_{0.05}$ due to the elastic recovery during unloading. Thus, this approach can be more reasonably implemented if the equation for evaluating the residual deformation by the residual indent depth is known.

In this regard, the authors of this article propose to estimate the average residual deformation when the ball is used as indenter by the ratio of the residual indent depth h to the ball radius R, i.e. $\psi^{\rm in}_{\rm res}=h/R$. Then, with a residual strain 0.0005, the equation wil be $h_{0.05}=0.0005{\rm R}$. The load $F_{0.05}$, which corresponds to $h_{0.05}$ can be found from (12):

$$F_{0.05} = 0.0005qR^2. (22)$$

On the other hand, if the equation (16) is used,

$$t_{0.05} = \left(\frac{0.0005R^2q}{a}\right)^{1/n}. (23)$$

Then from (17) and (23), it follows:

$$(HB_t)_{0.05} = a^{\frac{1}{n}} (0.0005q)^{\frac{n-1}{n}} \frac{R^{\frac{n-2}{n}}}{2\pi}.$$
 (24)

It should be noted that the same approach can be applied to determine the hardness at the yield strength by instrumented indentation. For this, it is necessary to consider that the residual deformation is equal to 0.002 = 0.2%. Then, by using equations, which are similar to (22) - (24) with $h_{0.2} = 0.2\%$.

= 0.002R, an equation for evaluating the hardness at the yield strength can be obtained:

$$(HB_t)_{0.2} = \frac{a^{\frac{1}{n}}(0.002q)^{\frac{n-1}{n}}R^{\frac{n-2}{n}}}{2\pi}.$$
 (25)

Another approach for evaluating the conditional hardness at the yield strength $(HB_t)_y$ was proposed by the authors of this paper in [28]. In this paper it was considered that at the initial stage of elastoplastic instrumented indentation the residual indent depth h_y is equal to the elastic component $(\alpha_{el})_y$ of the total elastoplastic displacement α_y . Under this condition it will be obtained

$$\alpha_{v} = h_{v} + (\alpha_{el})_{v}. \tag{26}$$

The total unrestored indent depth t_{v} is

$$t_{\nu} = h_{\nu} + \gamma (\alpha_{el})_{\nu} = h_{\nu} (1 + \gamma).$$
 (27)

Then, the conditional hardness at the yield strength $(HB_t)_y$ can be evaluated by the following equation, if (12), (17) and (27) are used:

$$(HB_t)_y = \frac{q}{2\pi(1+\gamma)}.$$
 (28)

In the particular case when $E_m = E_i$ and $\gamma = 0.5$, $(HB_t)_{\gamma}$ will be

$$(HB_t)_y = \frac{q}{3\pi}. (29)$$

The most reliable method to determine the maximum hardness or hardness at the ultimate strength $(HB_t)_u$ is to register the diagram " $HB_t - t/R$," which includes the maximum and subsequent decrease in hardness (see Fig. 6a).

If the diagram " $HB_t - t/R$ " cannot be recorded, then the primary indentation diagram " $F - \alpha$ " can be used to identify the inflection point b, which corresponds to the load F_b with the total displacement α_b , from which $(HB_t)_u$ can be evaluated. The point b is revealed more clearly in the indentation diagram with the logarithmic coordinates " $\ln F - \ln \alpha$." Other methods to identify b consist in determining the current values of $dF/d\alpha$ or the hardening pa-

rameter n. If the $\mathrm{d}F/\mathrm{d}\alpha$ becomes constant and the hardening parameter n is equal to 1, then this indicates that the point b is reached. The described methods of identifying the point b coordinates can be automated and graphically represented in the form of transformed diagrams " $\mathrm{d}F/\mathrm{d}\alpha - F$ " or "n-F".

Thus, the approaches to determining hardness at the elastic limit, hardness at the yield strength and hardness at the ultimate strength were described earlier. Each of these hardness characteristics can be determined at least by two methods. Table 2 shows the results of determining hardness characteristics in different ways for materials, which have different mechanical properties and strain hardening ability.

As follows from Table 2, for all presented materials $(HB_t)_{el}^* < (HB_t)_{0.05} < (HB_t)_{0.2}$. It is a consequence of greater hardening of the material when residual deformation is increased. The maximum hardness values $(HB_t)_u$, which is determined from the maximum diagrams " $HB_t - t/R$ " and from the $dF/d\alpha = const$, differ by no more than 3%. If the value of $(HB_t)_{0,2}$ and $(HB_t)_v$ is compared, their difference does not exceed 10%. However, in any case, the determination of these hardness characteristics by different methods and equations gives results that are more accurate. The described methods for determining E_m , $(HB_t)_{el}^*$, $(HB_t)_{0.05}$, $(HB_t)_{0.2}$, $(HB_t)_y$, $(HB_t)_u$ can be automated by using instrumented indentation, the indentation diagram " $F - \alpha$ " and the proposed equations.

CONCLUSION

Instrumented indentation is an effective mechanical test of the surface layer of materials. Ball indentation diagrams "load – indenter displacement" with loading and unloading curves contain important information about material resistance to loading at the elastic and elastoplastic deformation stages. These diagrams, which are converted to diagrams "indentation Brinell hardness HB_t – relative unrestored indent depth t/R," are similar and have a relation with tensile diagrams "conditional stress σ – relative elongation δ " and contain common characteristic zones and points from which stresses

Table 2. Determination results of the hardness characteristics $(HB_t)_{el}^*$, $(HB_t)_{0.05}$, $(HB_t)_{0.2}$, $(HB_t)_y$, $(HB_t)_u$ for different structural materials by ball instrumented indentation (R=0.5 mm)

Material	$\left(HB_{t}\right)_{el}^{*},\mathrm{N/mm^{2}},$ Eq. (20)	$(HB_t)_{0.05}, \mathrm{N/mm^2}, \ \mathrm{Eq.} \ (24)$	$(HB_t)_{0.2}, \mathrm{N/mm^2}, \ \mathrm{Eq.} \ (25)$	$\begin{array}{c} (HB_t)_{\mathcal{Y}},\mathrm{N/mm^2},\\ \mathrm{Eq.}\;(28) \end{array}$	$(HB_t)_u,\mathrm{N/mm^2}$ From the diagram	$(HB_t)_u$, N/mm ² From dF/d α
AMTs	296	328	359	349	465	451
15Kh1M1F	845	999	1126	1137	1610	1641
Steel 50	1573	1612	1760	1701	2158	2167
35KhVFYuA	1603	1716	2012	2159	3390	3402

and strains can be determined under both types of loading material.

The hardness characteristics at the elastic limit, at the yield strength and at the ultimate strength, which were determined by the instrumented indentation diagrams, make it more reasonable to establish its relationship with the elastic limit, the yield strength and the ultimate strength that were determined by the tensile diagrams.

REFERENCES

- Grodzinski P. Elastic and plastic hardness of hard materials / Nature. 1952. Vol. 169. N 4309. P. 925 – 926.
- Grodzinski P. Hardness testing of plastics / Plastics. 1953.
 N 18. P. 312 314.
- Kaley G. N. Device and method for microhardness evaluation with the estimation of indent depth / Advances in Research and Industrial Experience. — Russia: GOSINTI, 1967. N 18-67-1044/95 [in Russian].
- Kaley G. N. Results of microhardness evaluation with the estimation of indent depth / Machine Science. 1968. N 3. P. 105 [in Russian].
- USSR Pat. N 365622, Degtyarev V. I., Kurten L. I., Markovets M. P., Matyunin V. M., Plotnikov V. P. Method of ultimate strength evaluation, 1970 [in Russian].
- Markovets M. P., Matyunin V. M., Degtyarev V. I. Hardness diagrams as the indicator of materials mechanical properties / Proc. Int. Conf. "Research and Control of materials mechanical properties by non-destructive methods". — Russia, Volgograd, 1972 [in Russian].
- Degtyarev V. I., Matyunin V. M., Lagveshkin V. Ya. Automatic registration of hardness diagrams / MPEI researches. Moscow: MPEI, 1972. N 104. P. 86 89 [in Russian].
- Alekhin V. P., Berlin G. S., Isaev A. V. Method of materials micro indentation / Zavod. Lab. 1972. Vol. 38. N 4. P. 488 – 490 [in Russian].
- Bulychev S. I., Alekhin V. P., Shorshorov M. Kh., Ternovsky A. P., Shnyrev G. D. Young's modulus evaluation using instrumented indentation diagrams / Zavod. Lab. 1975. Vol. 41. N 11. P. 1137 – 1140 [in Russian].
- Bulychev S. I., Alekhin V. P., Shorshorov M. Kh., Ternovsky A. P. Materials mechanical properties evaluation using instrumented microindentation diagrams "load displacement" / Probl. Prochn. 1976. N 9. P. 79 83 [in Russian].
- Markovets M. P. Evaluation of metal mechanical properties by hardness. — Moscow: Mashinostroenie, 1979. — 191 p. [in Russian].
- Tangena A. G., Hurks G. A. M. The determination of stressstrain curves of thin layers using indentation tests / J. Eng. Mater. Technol. 1986. N 3. P. 230.
- Bulychev S. I., Alekhin V. P. Materials instrumented indentation test. Moscow: Mashinostroenie, 1990. 224 p. [in Russian].
- 14. **Oliver W. C., Pharr G. M.** Measurement of hardness and elastic modulus by instrumented indentation: Advances in understanding and refinements to methodology / J. Mater. Res. Soc. 2004. Vol. 19. N 1. P. 3 20.

- Oliver W. C., Pharr G. M. An improved technique for determining hardness and elastic modulus using load and displacement sensing indentation experiments / J. Mater. Res. 1992. Vol. 7. N 6. P. 1564 1583.
- Fedosov S. A., Peshek L. The application of microindentation methods for materials mechanical properties evaluation. — Moscow: Izd. MGU, 2004. — 98 p. [in Russian].
- Golovin Yu. I. Nanoindentation and its potential. Moscow: Mashinostroenie, 2009. — 312 p. [in Russian].
- Kovalev A. P. Common regularities if ball indentation and estimation of surface layers mechanical properties / Uprochn. Tekhnol. Pokryt. 2007. N 1. P. 36 – 41 [in Russian].
- Matyunin V. M. Indentation as the materials mechanical properties diagnostics method. Moscow: Izd. MPEI, 2015. 288 p. [in Russian].
- State Standard GOST R 8.748–2011. Metallic materials Instrumented indentation test for hardness and materials parameters. Part 1. Test method. — Moscow: Standartinform, 2013. — 28 p. [in Russian].
- State Standard GOST R 56232–2014. Stress strain curve evaluation using the ball instrumented indentation test. Moscow: Standartinform, 2015. 44 p. [in Russian].
- 22. State Standard GOST R 8.904–2015. Metallic materials. Instrumented indentation test for hardness and materials parameters. Part 2. Moscow: Standartinform, 2016. 30 p. [in Russian].
- State Standard GOST R 56474–2015. Space systems. Nondestructive control of materials and coatings mechanical properties by dynamic indentation. — Moscow: Standartinform, 2015. — 22 p. [in Russian].
- Hertz H. Über die Beruhrung fester elastischer Korper / Journal für die reine und angewanndte Mathematik. 1881. Bd. 92.
 S. 156 171 [in German].
- 25. Matyunin V. M., Marchenkov A. Yu., Abusaif N., Stasenko N. A. Evaluation of hardness tester elastic compliance for ball instrumented indentation / Zavod. Lab. Diagn. Mater. 2019. Vol. 85. N 4. P. 57 63 [in Russian].
- Drozd M. S., Matlin M. M., Sidyakin Yu. I. Engineering calculations for elastic-plastic contact strain. Moscow: Mashinostroenie, 1986. 224 p. [in Russian].
- 27. Matlin M. M., Mozgunova A. I., Kazankina E. N., Kazankin V. A. Methods of non-destructive evaluation of machines components strength characteristics. Moscow: Innovatsion-noe mashinostroenie, 2019. 246 p. [in Russian].
- Matyunin V. M., Marchenkov A. Yu., Volkov P. V. Yield stress evaluation using the ball indentation diagram / Zavod. Lab. Diagn. Mater. 2017. Vol. 83. N 6. P. 57 – 61 [in Russian].
- Hertz H. Über die Beruhrung fester elastischer Korper und über die Harte / Verhandlungen des Vereinis zur Beforderung des Gewerbefleifses. — Berlin, 1882. S. 174 – 175 [in German].
- 30. **Zaitsev G. P.** Hertz research and Brinell test / Zh. Tekhn. Fiz. 1949. Vol. 19. N 3. P. 336 346 [in Russian].
- Beckpaganbetov A. U., Matyunin V. M., Nemytov D. S. Hardness determination at the transition of elastic strain to elastoplastic strain / Zavod. Lab. Diagn. Mater. 2004. Vol. 70. N 6. P. 42 – 46 [in Russian].
- Shabanov V. M. Metals resistance for initial plastic deformation during ball indentation / Zavod. Lab. Diagn. Mater. 2008. Vol. 74. N 6. P. 63 – 69 [in Russian].